EPJ Web of Conferences **70**, 00007 (2014)
DOI: 10.1051/epjconf/20147000007

$W^{\pm}$ Z and Diboson physics at ATLAS

Nick Edwards[1], On behalf of the ATLAS Collaboration

[1] *University of Glasgow*

Abstract. A summary of recent results from the ATLAS experiment at the LHC in the field of $W^{\pm}$ Z and diboson physics is presented. Inclusive $W^{\pm}$ and Z production cross sections were measured differentially and compared to different PDF sets. The ratio of the total $W^{\pm}$ and Z cross section was used to measure the strange quark density in the light quark sea. The first measurement of tau polarisation made at a hadron collider is presented. Cross section measurements for the diboson processes $W^{\pm}\gamma$, $Z\gamma$, $W^{+}W^{-}$, $W^{\pm}Z$ and ZZ are presented. The diboson measurements are used to set limits on anomalous Triple Gauge Couplings; the results are consistent with the Standard Model values.

1 Introduction

$W^{\pm}$ and Z bosons are produced at a high rate at the LHC, and during LHC running in 2010 and 2011 the ATLAS experiment [1] has collected large statistics data samples of $W^{\pm}$ and Z events. Production of these bosons at hadron colliders is theoretically well understood, and has been calculated to NNLO. Measurements of $W^{\pm}$ and Z production thus give an important test of Quantum Chromodynamics (QCD). A crucial ingredient to the cross section calculations are the momentum distribution functions for the quarks in the proton (PDFs). Precise measurements of the cross sections thus give the ability to distinguish between predictions obtained using different PDF sets.

The large datasets collected by ATLAS in 2011 also allow the study of rarer process such as diboson production. In the absence of any direct beyond the standard model signals, probing the gauge structure of the electroweak theory is crucial to gain a hint of any new physics. Measurements of diboson processes gives access to the triple vector boson couplings.

A selection of the results obtained by ATLAS in the field of $W^{\pm}$, Z and diboson physics are presented here. All the results relate to data collected in pp collisions at a centre of mass energy of $\sqrt{s} = 7$ TeV, collected in 2010 and 2011.

2 Inclusive $W^{\pm}$ and Z measurements

The production cross sections for the inclusive Drell-Yan processes $W \to \ell\nu$ and $Z \to \ell\ell$ are measured in the electron and muon decay channels using a dataset corresponding to an integrated luminosity of 35pb^{-1} collected in 2010 [2]. For the case of $Z \to \ell\ell$ the cross section is measured differentially as a function of the Z boson rapidity, y_Z; for $W \to \ell\nu$ the cross sections are measured as a function of the pseudo-rapidity of the charged lepton, η_ℓ. Figures 1 and 2 show the measured cross sections for the Z, W^{+} and W^{-}, respectively. A comparison is made with the predictions using the JR09, ABKM09,

HERAPDF1.5 and MSTW08 NNLO PDF sets. The level of precision of the ATLAS measurements is already sufficient to discriminate between the PDF sets. The observed dependencies on y_Z and η_ℓ are generally well described by the predictions. However, some deviations are observed, for example the Z cross section at central rapidities is under-predicted when using the JR09 PDF set, and the $W^\pm$ and Z cross sections at high y_Z and η_ℓ are over-predicted using ABKM09.

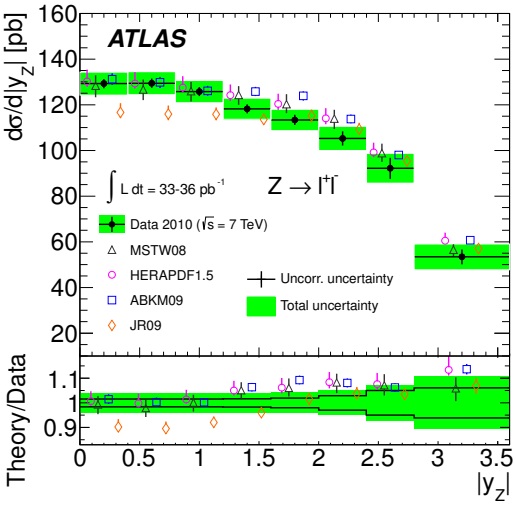

Figure 1. Differential $d\sigma/d|y_Z|$ cross section measurement for $Z \to \ell\ell$ compared to NNLO theory predictions using various PDF sets [2]. The kinematic requirements are $66 < m_{ll} < 116$ GeV and $p_{T,\ell} > 20$ GeV. The ratio of theoretical predictions to data is shown at the bottom. Theoretical points are displaced for clarity within each bin.

Since the production of $W^\pm$ and Z bosons is independent of the decay lepton flavour, the ratio of the electron to the muon channel cross sections in $W^\pm$ or Z decays gives a measurement of the ratios of the branching fractions. Figure 3 shows the observed ratios; they are consistent with the current world average values and the Standard Model prediction.

The ratio of the $W^\pm$ and Z cross sections is sensitive to the density of the strange quark in the proton, since the strange quark contributes to $W^\pm$ and Z production through the non-identical sub-processes $s\bar{s} \to Z$ and $sc \to W$ [3]. A NNLO fit to ATLAS $W^\pm$ and Z data, together with ep data from HERA, was carried out to extract the ratio of the strange-quark to the anti-down-quark content in the sea, given by $r_s = 0.5(s + \bar{s})/\bar{d}$ at $Q^2 = 1.9$ GeV^2, $x = 0.023$. The result, shown in Figure 4, is consistent with a flavour symmetric sea at low Bjorken x.

A measurement of the τ polarisation was performed using $W \to \tau\nu$ decays [4]. The Standard Model predicts that the W^- couples exclusively to left-handed τ^- and that the W^+ couples exclusively to right-handed τ^+. The polarisation is defined as $P_\tau = (\sigma_R - \sigma_L)/(\sigma_R + \sigma_L)$ for the production of τ^-. The angle θ between the τ direction of flight and the hadronic decay products in the τ rest frame is the primary observable sensitive to the polarisation. Unfortunately this is not directly accessible experimentally as the τ momentum reconstruction is limited due to the multiple unobserved neutrinos in the event. However, the 'charged asymmetry', the energy asymmetry between the charged and the neutral decay products in hadronic τ decays, denoted Υ, retains sensitivity to the polarisation of the τ. Templates from simulation of left and right-handed τ are fitted to the observed Υ distribution in

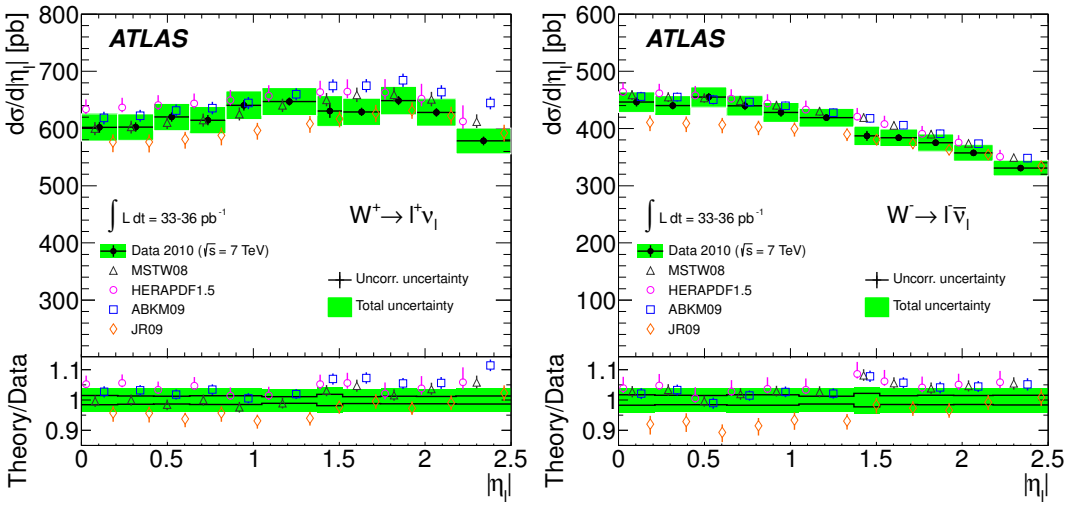

Figure 2. Differential $d\sigma/d|\eta_\ell|$ cross section measurements for $W \to \ell\nu$ for W^+ (top) W^- (bottom), compared to the NNLO theory predictions using various PDF sets [2]. The kinematic requirements are $p_{T,\ell} > 20$ GeV, $p_{T,\nu} > 25$ GeV and $m_T > 40$ GeV. The ratio of theoretical predictions to data is shown at the bottom. Theoretical points are displaced for clarity within each bin.

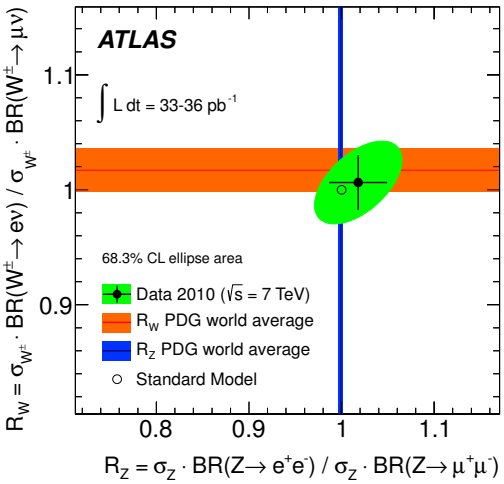

Figure 3. The measurement of the electron-to-muon cross section ratios in the $W^\pm$ and the Z channels [2]. The vertical (horizontal) band represents the uncertainty of the corresponding Z ($W^\pm$) branching fractions based on the current world average data. The green ellipse illustrates the 68% CL for the correlated measurement of R_W and R_Z, while the error bars correspond to the one-dimensional uncertainties of either R_W or R_Z , respectively.

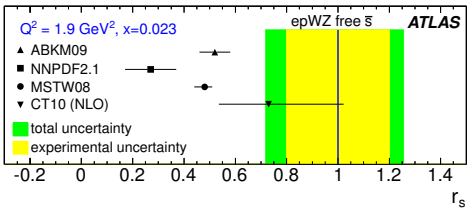

Figure 4. Measurement and predictions for the ratio $r_s = 0.5(s + \bar{s})/\bar{d}$, at $Q^2 = 1.9$ GeV^2, $x = 0.023$. The points show global fit results using the PDF sets as quoted. The bands show the measurement by ATLAS [3]; the inner band shows the experimental uncertainty and the outer band shows the total uncertainty.

order to extract the polarisation; this is shown in Figure 5. The observed polarisation is found to be $P_\tau = -1.06 \pm 0.04\ (\text{stat})^{+0.05}_{-0.07}\ (\text{syst})$. This is compatible with the Standard Model expectation of - 1, and is the first measurement of the τ polarisation at a hadron collider.

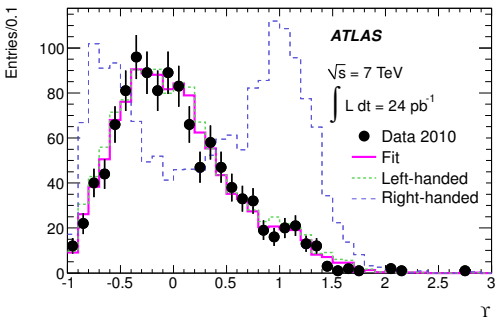

Figure 5. Distribution of the charged asymmetry variable Υ in $W \to \tau\nu$ decays [4]. The distribution observed in data is shown as solid points. Simulated templates for left-handed and right-handed tau decays, including signal and background contributions, are shown as green short dashed- and blue long dashed- lines, respectively. The best fit resulting from maximizing the likelihood is plotted as a bold pink line.

3 Diboson Physics

Measurements of diboson processes allow precise tests of the structure of the Electroweak theory. Diboson production is also sensitive to new physics, either through resonant production of new particles or through anomalous Triple Gauge couplings (aTGCs). Deviations of the TGCs from the Standard Model prediction could occur from a composite structure of the $W^\pm$ and Z, or from the presence of new particles decaying to $W^\pm$ or Z. In addition, direct W^+W^- and ZZ production constitutes the major irreducible background in the corresponding Higgs boson decay channels, and are thus crucial to understand for Higgs boson studies.

The diboson processes considered here are $W^\pm\gamma$, $Z\gamma$, W^+W^-, $W^\pm Z$ and ZZ. Each of these give access to a different set of aTGCs. Table 1 summarises the couplings probed, the associated coupling parameters, and the diboson channels which are sensitive to them. Any anomalous TGCs would

Coupling	Parameters	Channel
$WW\gamma$	Λ_γ, Δk_γ	W^+W^-, $W^\pm\gamma$
WWZ	Λ_Z, Δg_1^Z, Δk_Z	W^+W^-, $W^\pm Z$
$ZZ\gamma$	h_3^Z, h_4^Z	$Z\gamma$
$Z\gamma\gamma$	h_3^γ, h_4^γ	$Z\gamma$
ZZZ	f_4^Z, f_5^Z	ZZ
$Z\gamma Z$	f_4^γ,f_5^γ	ZZ

Table 1. Summary of the different aTGC couplings probed. In each case the parameters used to describe the couplings and the decay channels sensitive to the coupling are given.

manifest as increased cross sections, particularly at high centre of mass energies and small scattering angles, so observables such as the mass and transverse momentum of the boson system are particularly sensitive to aTGCs. When parameterising the coupling, form factors are applied to the coupling parameter to preserve unitarity at high centre of mass energies. The typical choice of form factor is $f' = f/(1 + \hat{s}/\Lambda^2)^n$, where n gives the 'strength' of the form factor and Λ is the new physics energy scale.

The $W^\pm\gamma$ and $Z\gamma$ cross sections were measured using a dataset corresponding to an integrated luminosity of 1fb^{-1} collected in 2011, selecting events where the boson decays to electrons or muons [5]. The cross sections, measured differentially as a function of E_T^γ are shown in Figure 6. Two measurements are made: an exclusive measurement where any event containing a hard jet with $p_T > 30$ GeV is rejected, and an inclusive measurement where no such requirement is made. The measurements are compared to the NLO prediction of MCFM [6]. In general the predictions agree well with the data, although in the inclusive $W^\pm\gamma$ cross section the prediction under-estimates the data in the higher E_T^γ bins.

The photon spectra in $W^\pm\gamma$ and $Z\gamma$ events are sensitive to aTGCs, particularly at high photon energies. The $W^\pm\gamma$ process is sensitive to a modification of the existing $WW\gamma$ coupling, which can be parameterised with two parameters, $\Delta\kappa_\gamma$ and λ_γ. The $Z\gamma$ process is sensitive to the $ZZ\gamma$ and $Z\gamma\gamma$ couplings, both of which are forbidden in the SM; these may be parameterised by four couplings h_3^γ, h_4^γ, h_3^Z and h_4^Z. The measured cross sections for $E_\gamma > 100$ GeV are used to set limits on the couplings. The resulting limits are shown in Figure 7. No evidence for new physics is seen, and the limits set are compatible with those obtained from LEP and the Tevatron.

The W^+W^- production cross section was measured using the full 2011 dataset, corresponding to an integrated luminosity of 4.7 fb^{-1} [7], using events where both $W^\pm$ bosons decay to electrons or muons. In order to distinguish the signal from the large Drell-Yan and $t\bar{t}$ backgrounds, events are required to have large missing transverse energy and not to have any high transverse momentum jets. The cross section was measured to be 53.4 ± 2.1 (stat) ± 4.5 (syst) ± 2.1 (lumi) pb, to be compared with the NLO Standard Model prediction of 45.1 ± 2.8 pb (calculated using MC@NLO [8] and PDF set CT10 [9]). The observed transverse mass distribution is shown in Figure 8. W^+W^- production is sensitive to anomalous couplings in the $WW\gamma$ and WWZ vertices. Assuming that the couplings arise from dimension-6 operators and that electroweak symmetry breaking occurs via a light Standard Model Higgs (the so called "LEP assumption" [10]) the anomalous coupling can be parameterised by three parameters: Δg_1^Z, Δk_Z and Λ_Z. Limits are set using 1 fb^{-1} of the dataset [11] by performing a binned likelihood fit on the leading lepton p_T distribution, shown in Figure 9. The resulting limits are shown in Figure 10. The sensitivity of this result is significantly greater than that of the Tevatron due

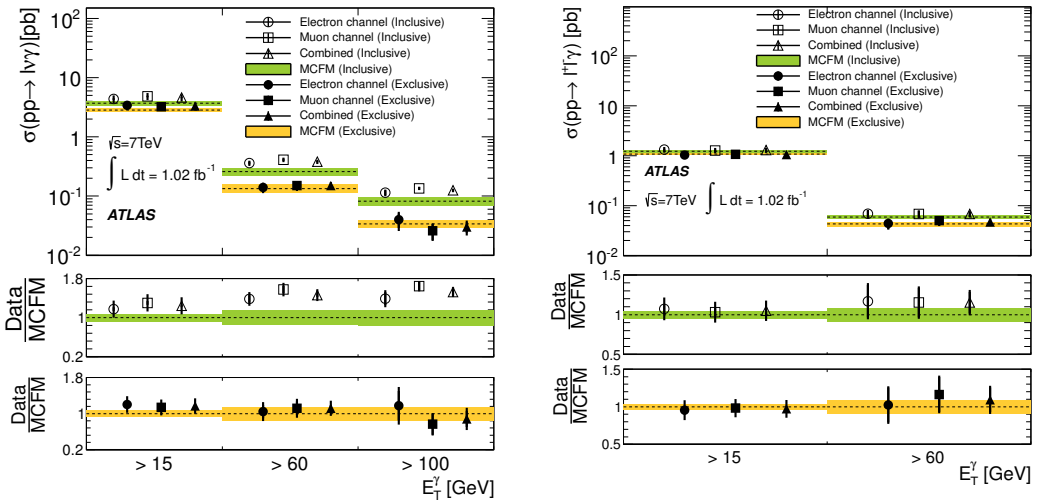

Figure 6. The measured cross section for $W^{\pm}\gamma$ (top) and $Z\gamma$ (bottom) production [5] together with the NLO SM model prediction obtained using MCFM [6]. The measurements are performed in different $E_{T,\gamma}$ bins. For a better comparison to SM predictions the events are analyzed both inclusively, with no requirements on the recoil system (shown with open markers and green bands), and exclusively, requiring there be no hard jet (closed markers and yellow bands). The lower plots show the ratio between the data and the prediction of the MCFM generator.

to the higher centre-of-mass energy and higher W^+W^- production cross section, and is comparable with the combined results from LEP.

The $W^{\pm}Z$ production cross section was measured using a dataset corresponding to 1.02 fb^{-1} collected in 2011, using events where both bosons decay to electrons or muons [12]. Events were selected by requiring three isolated high p_T leptons, two of which form a same-flavour opposite-sign pair with an invariant mass withing 10 GeV of the Z mass, and by requiring large missing transverse momentum. 71 events passed these requirements, with a background estimation of 12.1 ± 1.4 (stat) $^{+4.1}_{-2.0}$ (syst). The observed $W^{\pm}Z$ transverse mass distribution of events passing the selection is shown in Figure 11. The measured cross section was 20.5 $^{+3.1}_{-2.8}$ (stat) $^{+1.4}_{-1.3}$ (syst) $^{+0.9}_{-0.8}$ (lumi) pb, to be compared with the Standard Model NLO prediction of 17.3 $^{+1.3}_{-0.8}$ pb. $W^{\pm}Z$ production is sensitive to anomalous couplings in the WWZ vertex, which as above is described by Δg_1^Z, Δk_Z and Λ_Z. Limits are set using the number of observed events only; the resulting limits are shown in Figure 12.

The ZZ production cross section was measured using the full 2011 dataset of 4.7 fb^{-1}, using the decay channels $ZZ \to \ell\ell\ell'\ell'$ [13] and $ZZ \to \ell^-\ell^+\nu\bar{\nu}$ [14]. In the $ZZ \to \ell^-\ell^+\nu\bar{\nu}$ channel, events are selected by requiring a pair of opposite-sign same-flavour high p_{T} isolated leptons with invariant mass within 15 GeV of the Z mass, large $E_{\mathrm{T}}^{\mathrm{miss}}$ and no high p_{T} jets. Applying these requirements, 78 events were observed with a background estimation of 40.7 ± 4.3 (stat) ± 3.7 (syst). Figure 13 shows the observed transverse mass distribution of the dilepton+E_T^{Miss} system in events passing the selection. The measured total ZZ production cross section measured using this channel was 5.4 $^{+1.3}_{-1.2}$ (stat) $^{+1.4}_{-1.0}$ (syst) ± 0.2 (lumi) pb, which is compatible with the Standard Model NLO prediction of 6.5 $^{+0.3}_{-0.2}$ pb.

In the $ZZ \to \ell\ell\ell'\ell'$ channel, events are selected by requiring exactly four high p_{T} leptons, forming two opposite-sign same-flavour pairs. Ambiguities in pairing are resolved by choosing the pairing which minimises the sum of the differences between each pair and the PDG Z boson mass. Applying

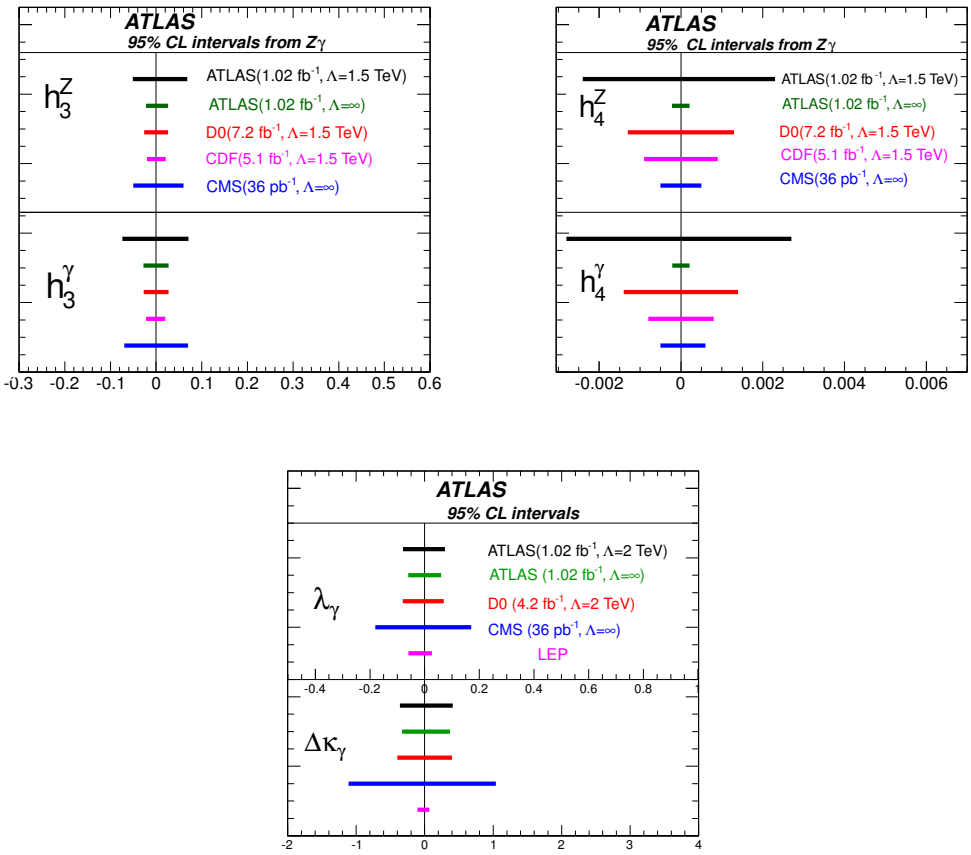

Figure 7. The 95% C.L. intervals for anomalous couplings from ATLAS, D0, CDF, CMS and LEP [5]. The top figure shows the limits for the neutral aTGCs h_3^γ and h_3^Z, obtained from $Z\gamma$ events. The middle figure show the limits on the neutral aTGCs h_4^γ and h_4^Z, obtained from $Z\gamma$ events. The bottom plot shows the limits on the charged aTGCs $\Delta\kappa_\gamma$ and λ_γ (bottom) from $W^\pm\gamma$ events. Luminosities and the new physics scale parameter Λ are shown. The sensitivity of the LEP data to neutral aTGCs is much smaller than that of the hadron colliders; therefore the LEP results have not been included.

these requirements, 62 events were observed, with a background expectation of 0.7 $^{+1.3}_{-0.7}$ (stat) $^{+1.3}_{-0.7}$ (syst) events (estimated from data). The invariant mass of the leading lepton pair versus the invariant mass of the subleading lepton pair in selected events is shown in Figure 14. The four lepton invariant mass distribution is shown in Figure 15. The measured total ZZ production cross section measured using this channel is 7.2 $^{+1.1}_{-0.9}$ (stat) $^{+0.4}_{-0.3}$ (syst) ± 0.3 (lumi) pb. The results from the $ZZ \to \ell^-\ell^+\nu\bar{\nu}$ and $ZZ \to \ell\ell\ell'\ell'$ channels have not yet been combined; the two measurements give two measurements of the same quantity. A comparison of the two measurements and the Standard Model prediction are shown in Figure 16.

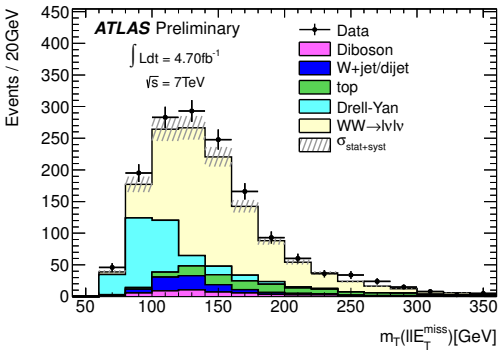

Figure 8. Distributions of the transverse mass of the dilepton+E_T^{Miss} system for the W^+W^- candidates [7]. The points represent data and the stacked histograms the signal expectation and background estimates. The histogram shapes are MC-based except for the W+jets background contribution, which is obtained from a data-driven method. The estimated uncertainties are shown as hatched bands (stat+syst).

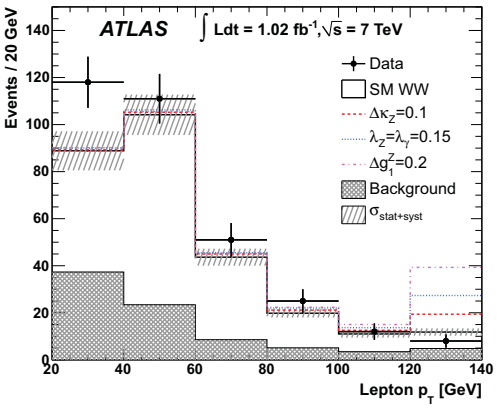

Figure 9. The p_{T} distribution of the highest-p_{T} charged lepton in W^+W^- final states [11]. Shown are the data (dots), the background (shaded histogram), Standard Model W^+W^- (solid histogram), and different W^+W^- anomalous couplings added to the background (various line styles). The last bin corresponds to $p_{\mathrm{T}} > 120$ GeV.

ZZ production is sensitive to the ZZZ and $Z\gamma Z$ vertices; both of these are forbidden in the Standard Model. The couplings can be parameterised with four parameters: f_4^γ,f_5^γ,f_4^Z, and f_5^Z. Limits are set using the first 1.02fb^{-1} of the dataset, using the total number of observed events [15]. No evidence for TGC couplings is observed, and the resulting limits are shown in Figure 17. The limits are comparable to, or more stringent than limits set by LEP and the Tevatron.

4 Conclusions

A selection of recent $W^\pm$, Z and diboson measurements made by the ATLAS experiment were presented. Measurements of the inclusive $W^\pm$ and Z production cross sections were compared to pre-

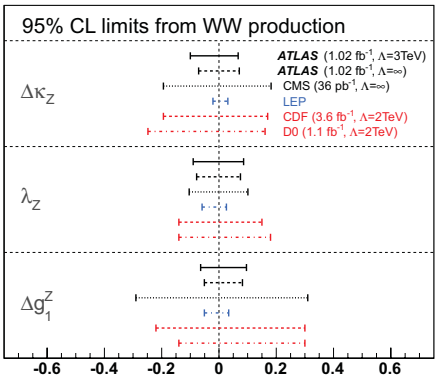

Figure 10. Anomalous TGC limits from ATLAS, D0 and LEP (based on the LEP scenario) and CDF and CMS (based on the HISZ scenario), as obtained from W^+W^- production measurements [11].

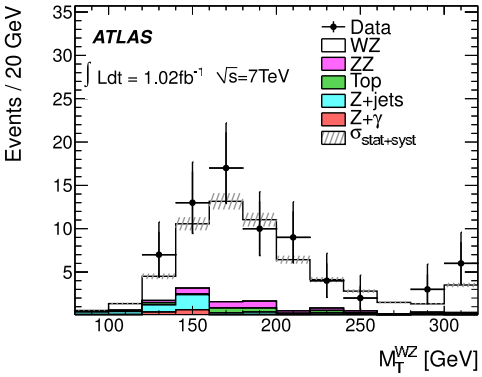

Figure 11. The $W^{\pm}Z$ transverse mass distribution after all cuts for $W^{\pm}Z$ candidates [12]; the last bin is the overflow bin. The shaded bands indicate the total statistical and systematic uncertainties on the MC prediction.

dictions from different PDF sets. The level of precision of the measurement is great enough to allow discrimination between the predictions of different PDF sets. The ratio of the total $W^{\pm}$ and Z cross section is used to determine the strange quark density in the light quark sea; the result favours a flavour symmetric light quark sea. The tau polarisation in $W \to \tau\nu$ decays is measured, and is found to be consistent with the Standard Model prediction. Cross section measurements for the diboson processes $W^{\pm}\gamma$, $Z\gamma$, W^+W^-, $W^{\pm}Z$ and ZZ were presented. The diboson measurements were used to set limits on anomalous Triple Gauge Couplings; the results are consistent with the Standard Model. To date, ATLAS has collected more than twice as much data in 2012 as in 2011, at a higher centre of mass energy of $\sqrt{s} = 8$ TeV. This larger dataset will allow further measurements with refined precision, particularly for the diboson measurements which are limited by statistical uncertainties.

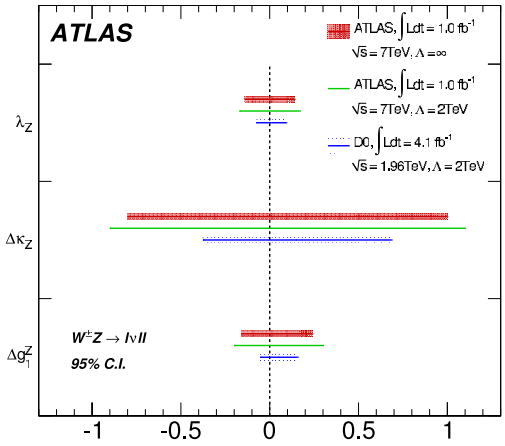

Figure 12. 95% C.I. for anomalous couplings from ATLAS and D0 experiments [12]. ATLAS limits are extracted from a fit to the cross section while the D0 limits are extracted from a fit to the $p_T(Z)$ spectrum. Luminosities, centre-of-mass energy and cut-off Λ are shown.

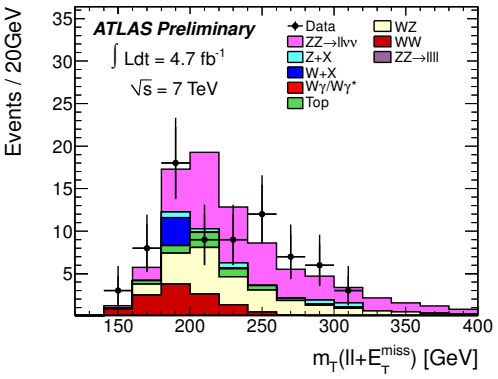

Figure 13. Transverse mass of the dilepton+E_T^{Miss} system in events passing the $ZZ \to \ell^-\ell^+\nu\bar{\nu}$ event selection [14]. The histograms show the predictions from Monte Carlo for the different contributions.

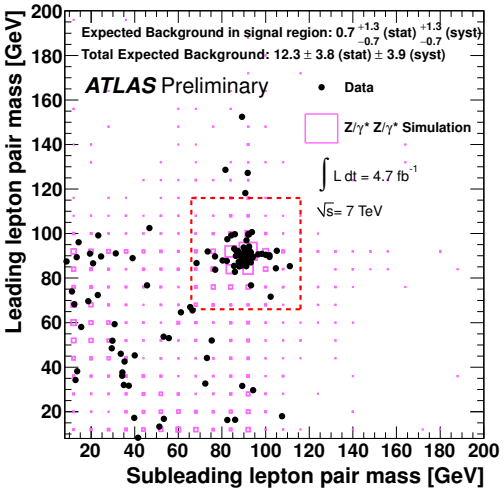

Figure 14. Invariant mass of the leading Z candidate versus the invariant mass of the subleading Z candidate in events passing the $ZZ \to \ell\ell\ell'\ell'$ selection [13]. The events observed in the data are shown as solid circles and the signal prediction from simulation as pink boxes. The large dashed red box indicates the signal region defined by the ZZ fiducial cuts on the Z candidate masses. Contributions from events with one or both Z bosons off-shell are also seen.

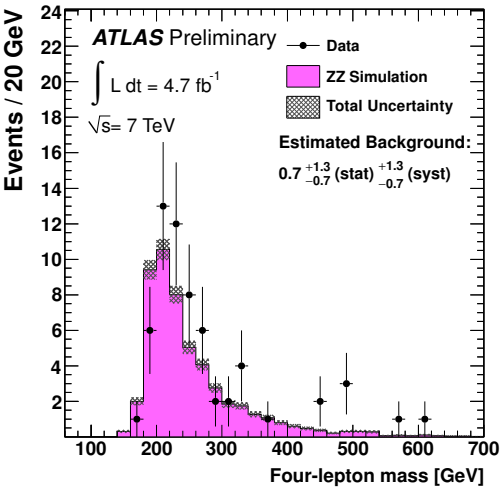

Figure 15. The four-lepton invariant mass for events passing the $ZZ \to \ell\ell\ell'\ell'$ selection [13]. The points are data and the histogram shows the signal prediction from simulation, normalized to the luminosity of the data. The grey band indicates the combined statistical and systematic uncertainty on the signal prediction.

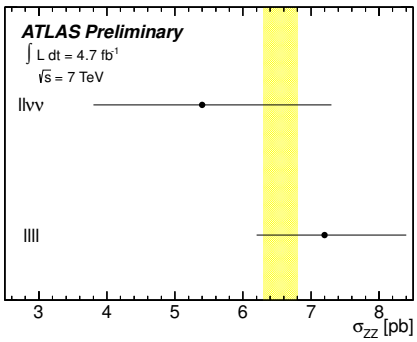

Figure 16. Comparison of total cross sections measured by the $ZZ \to \ell\ell\ell'\ell'$ and $ZZ \to \ell^-\ell^+\nu\bar{\nu}$ analyses with the theory prediction (yellow band) [14].

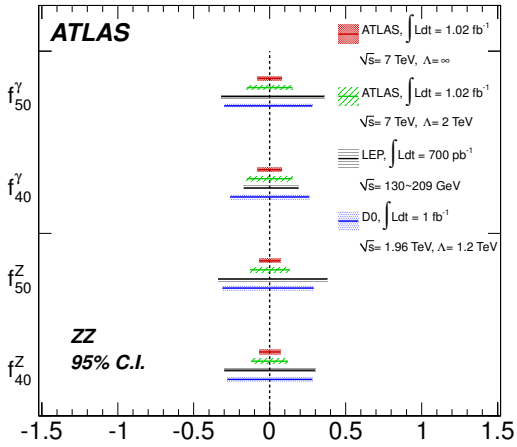

Figure 17. Anomalous nTGC 95% confidence intervals from ATLAS, LEP and Tevatron experiments. Luminosities, centre-of-mass energy and cut-off Lambda for each experiment are shown [15].

References

[1] ATLAS Collaboration, *The ATLAS Experiment at the CERN Large Hadron Collider*, JINST **3** (2008) S08003.

[2] ATLAS Collaboration, *Measurement of the inclusive $W^{\pm}$ and Z/γ cross sections in the electron and muon decay channels in pp collisions at $\sqrt{s}$ = 7 TeV with the ATLAS detector*, Phys.Rev. **D85** (2012) 072004, arXiv:1109.5141 [hep-ex].

[3] ATLAS Collaboration, *Determination of the strange quark density of the proton from ATLAS measurements of the $W \to \ell\nu$ and $Z \to \ell\ell$ cross sections*, Phys.Rev.Lett. **109** (2012) 012001, arXiv:1203.4051 [hep-ex].

[4] ATLAS Collaboration, *Measurement of τ polarization in $W \to \tau\nu$ decays with the ATLAS detector in pp collisions at $\sqrt{s}$ = 7 TeV*, Eur.Phys.J. **C72** (2012) 2062, arXiv:1204.6720 [hep-ex].

[5] ATLAS Collaboration, *Measurement of $W^{\pm}\gamma$ and $Z\gamma$ production cross sections in pp collisions at $\sqrt{s}$ = 7 TeV and limits on anomalous triple gauge couplings with the ATLAS detector*, arXiv:1205.2531 [hep-ex].

[6] J. Campbell, K. Ellis, and C. Williams, *Vector Boson Pair Production at the LHC*, FERMILAB-PUB-11-182-T **000** (2011) 035, arXiv:1105.0020v1[hep-ph].

[7] ATLAS Collaboration, *Measurement of the W+W- Production Cross Section in Proton-Proton Collisions at sqrt(s) = 7 TeV with the ATLAS Detector*, ATLAS-CONF-2012-025, Mar, 2012.

[8] S. Frixione and B.R. Webber, *Matching NLO QCD Computations and parton shower simulations*, J. High Energy Phys. **0206** (2002) 029.

[9] H. -L. Lai, M. Guzzi, J. Huston, Z. Li, P. M. Nadolsky, J. Pumplin and C. -P. Yuan, *New parton distributions for collider physics*, Phys. Rev. D **82** (2010) 074024, arXiv:hep-ph/1007:2241.

[10] K. Hagiwara, S. Ishihara, R. Szalapski, and D. Zeppenfeld, *Low-energy effects of new interactions in the electroweak boson sector*, Phys.Rev. **D48** (1993) 2182–2203.

[11] ATLAS Collaboration, *Measurement of the WW cross section in sqrt(s) = 7 TeV pp collisions with the ATLAS detector and limits on anomalous gauge couplings*, Phys.Lett. **B712** (2012) 289–308, arXiv:1203.6232 [hep-ex].

[12] ATLAS Collaboration, *Measurement of the WZ production cross section and limits on anomalous triple gauge couplings in proton-proton collisions at sqrt(s) = 7 TeV with the ATLAS detector*, Phys.Lett. **B709** (2012) 341–357, arXiv:1111.5570 [hep-ex].

[13] ATLAS Collaboration, *Measurement of the total ZZ production cross section in the four-lepton channel with 4.7 fb^{-1} of ATLAS data*, ATLAS-CONF-2012-026, Mar, 2012.

[14] ATLAS Collaboration, *Measurement of the ZZ production cross section in the llvv channel in proton-proton collisions at sqrt(s)=7 TeV with the ATLAS detector*, ATLAS-CONF-2012-027, Mar, 2012.

[15] ATLAS Collaboration, *Measurement of the ZZ production cross section and limits on anomalous neutral triple gauge couplings in proton-proton collisions at $\sqrt{s}$ = 7 TeV with the ATLAS detector*, Phys.Rev.Lett. **108** (2012) 041804, arXiv:1110.5016 [hep-ex].